# Advances in Photorefractive Polymers and Applications

P.-A. Blanche[1], B. Lynn, R. A. Norwood, N. Peyghambarian
College of Optical Sciences, The University of Arizona, Tucson AZ USA 85721.

## ABSTRACT

Photorefractive (PR) polymers change their index of refraction upon illumination through a series of electronic phenomena that makes these materials one of the most complex organic systems known. The refractive index change is dynamic and fully reversible, making PR materials very interesting for a large variety of applications such as holography and 3D display. In order to improve the recording speed and achieve videorate for our stereographic display application, we have introduced a new type of electrode geometry where the anode and cathode are in the same plane and are shaped as interpenetrating combs. This type of electrode geometry does not require the sample to be tilted with respect to the writing beams to record the hologram, which is a significant advantage. To monitor the highly non-homogeneous field resulting from this configuration, we used a multiphoton microscope to directly observe the chromophore orientation in situ upon the application of an electric field. Most recently, we developed a fast repetition rate laser (10kHz) where the pulse width can be adjusted from microseconds to milliseconds so that, in conjunction with a ns Q-switched Nd:YAG laser and an externally chopped CW laser, the diffraction efficiency of the material could be measured over 9 orders of magnitude. This measurement helps us better understand the mechanism of grating buildup inside photorefractive polymers.

**Keywords:** Holography, Photorefractive polymer, 3D display.

## 1. INTRODUCTION

Holographic stereography, or integral image holography, bridges the gap between two-view stereograms and the data-heavy hologram on the quest for 3D video displays. These systems holographically record the directionality of light for a discrete series of viewing locations, providing static and motion parallax without having to resort to direct fringe computation, transmission, and display.[1] They are also inherently amenable to the recording of real scene footage taken from multiple viewpoints. As the number of distinct viewing locations or views increases, the reproduced scene begins to closely approximate the original scene. This eliminates the vergence-accommodation conflict which occurs when the eyes focus on the screen but converge to the perceived location of the object, often causing accelerated fatigue and discomfort.[2] Utilizing photorefractive polymer as the recording medium in this type of display opens the door to eye-wear free, real-time updating holographic displays.

Improvements in photorefractive polymers have advanced this technology from a small, slowly refreshing proof-of-concept system to one that is nearing its premiere as a truly video-rate holographic display. Previous work has focused on optimizing the diffractive response of the devices to respond to 6 ns pulses delivering 200 mJ per pulse at a 50 Hz repetition rate while reducing the absorption of the material itself in the blue region to support full-color image reconstruction.[3] These improvements enabled the recording of a 300 mm×150 mm display in less than 8 seconds and full-color reconstruction with a color gamut extending beyond the NTSC CIE color space.[4]

Progress toward faster refresh rates was previously limited by a combination of the need to improve the sensitivity of the PR polymer to the recording intensity and the availability of current laser technology, which fell short of the need for 532 nm wavelength range pulsed laser with tens of millijoules per pulse and kHz repetition rates supporting video-rate recording. Several developments have been made by our group in these directions with the introduction of a new electrode geometry that allows for symmetric configuration of the recording beams,[5] and more recently the real-time imaging of the chromophore alignment through multiphoton microscopy.[6]

Lately, we developed a new single mode fiber based laser to enable the characterization and optimization of the PR polymer devices across a previously inaccessible region of pulse lengths between the regular 6 ns q-switched pulse and a 1 ms externally chopped high power CW beam. This intermediate region is very important to study from an application

---

[1]  pablanche@optics.arizona.edu

point of view since we have observed that the efficiency and sensitivity of the material at nanoseconds or milliseconds change by orders of magnitude. Understanding how the PR behavior changes with pulse width while conserving the energy delivered is critical to determine the best mode of operation in applications such as our holographic 3D display, where videorate requires the writing of 10,000 hogels per second.

## 2. EXPERIMENTAL SECTION

For conventional holographic materials, such as silver halide and photopolymers, the diffraction efficiency response is invariant with the pulse width of the writing laser and only depends on pulse energy. However at very small pulse temporal width and large peak power, this law breaks down, a phenomenon that is known as the "reciprocity failure".[7] This failure occurs because of the specific chemistry happening in the material: either latent image formation such as in silver halide or molecular polymerization in photopolymer and photoresin.[8] We observed a similar behavior for photorefractive polymers when using a nanosecond pulse laser compared to CW recording. We carried out a study of the diffraction efficiency according to the temporal pulse width of the writing beams over 9 orders of magnitude, and linked the observation to the PR mechanism.

To do so, we built a specific laser source in which the pulse width can be tuned. We used a MOPA configuration (master oscillator power amplification), where a CW IR telecom diode laser is chopped into pulses by a Pockels cell. The pulses are then re-amplified outside the cavity by two diode pumped fiber amplifiers. The IR pulse is then converted into 532 nm with a frequency doubling crystal and injected into a four wave mixing setup to record a diffraction grating in the sample. To be sure the grating is recorded with one single pulse, another Pockels cell is used to trigger a temporal window, passing a single pulse. A 633nm HeNe laser is used to read the grating and to measure the diffraction efficiency.

The pulsed fiber laser characteristics are:
- Energy per pulse: up to 100 µJ/pulse
- Pulse temporal width: from 250 ns to 250 µs
- Repetition rate: up to 10kHz
- Coherence length: 1cm

In addition to this new fiber laser, a regular Q-switched pulsed Nd:YAG laser (InnoLas SpitLight) with 6ns pulse duration was used to extend the measurement in the shorter pulse width region. As for longer pulse width, the beam from a CW Coherent Verdi V18 laser was externally chopped with a Pockels cell to achieve 1.5ms to 1s exposure times. Overall, with these three lasers, we were able to explore 9 orders of magnitude in pulse width time. It has to be noted that for each measurement, the pulse average energy was kept constant at 30 mJ/cm$^2$. However, the compression in time (from 1 s to 6 ns) means that the peak power varied by the same factor with 30 mW/cm$^2$ for the 1 second pulse and 5 GW/cm$^2$ for the 6 nanosecond pulse.

The PR polymer we used for this study is based on polyacrylic-tetraphenyldiaminobiphenyl (PATPD)[9] where carbaldehyde aniline (CAAN) was attached to the PATPD copolymer chain in a ratio of 10:1 (TPD:CAAN). This modification brings two advantages: first it increases the shelf life of the device by preventing phase separation; second, it increases the loading limit of the chromophore. The chromophore we used is fluorinated dicyanostyrene 4-homo-piperidino benzylidine malononitrile (FDCST). The plasticizer was benzyl butyl phthalate (BBP), and the sensitizer was [6,6]-phenyl-C61-butyric acid methyl ester (PCBM). The ratio of the component was TPD:CAAN/FDCST:BBP:PCBM (56.23:33.74:9.84:0.2 wt%). Sample was formed by melt pressing the compound between two transparent indium tin oxide (ITO) electrodes on glass to a thickness of 100 µm given by glass bead spacers. In addition, a 10 µm amorphous polycarbonate (APC) layer was spin casted on one electrode to reduce the risk of dielectric breakdown. We have seen in the past that such a layer influences both the dynamics and the efficiency of PR devices, slowing down and reducing the overmodulation voltage in four wave mixing experiment.[10]

The single pulse diffraction efficiency was measured using a non-degenerated four wave mixing setup, of which detailed description is given elsewhere.[11] To ensure the short pulses are delivered at the same time and interfere over their entire length in the material (a 6 ns pulse is 2 meters long), both arms of the four wave mixing setup were equalized by a delay line The writing beams were provided by one of the three lasers described here above. The probe beam was a CW HeNe at 633 nm with intensity set low enough to not perturb the recorded grating. The maximum diffraction efficiency measurement over 9 orders of magnitude of temporal pulse width are presented in figure 1. It is essential to note that the PR grating was recorded using *a single pulse* excitation. Single pulse writing is very important since the phase is kept

constant during the recording, which is not necessarily the case when multiple pulses are used. This is due to the mechanical vibration or thermal phenomenon that can modify the path length of the two interfering beams in between two pulses. Vibration and thermal effects are too slow to have an impact during the short duration of a single pulse below 0.1 ms. When the phase between the two beams is perturbed, the diffraction efficiency decreases because the intensity pattern is not stable during the recording. Single pulse recording is immune from that type of error. When the pulse temporal width is larger than 0.1 ms, mechanical vibration, acoustic vibration, and thermal fluctuation can modify the phase during the recording. To prevent these perturbations, our setup was assembled on an air floating table and kept inside an enclosure.
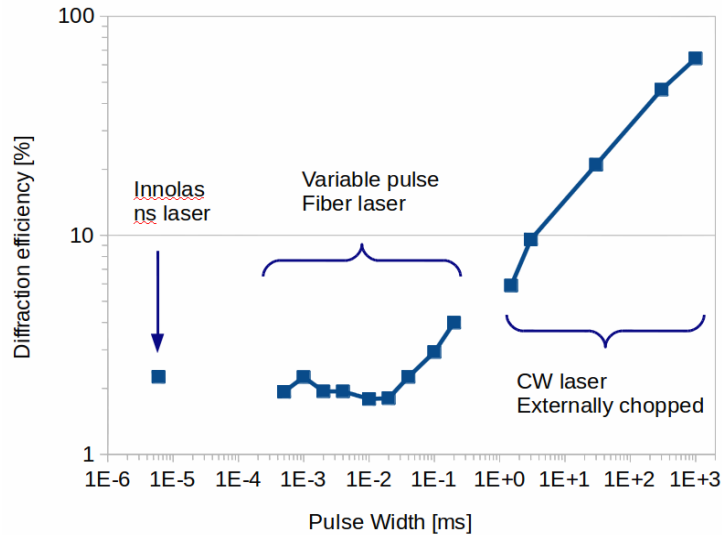


Figure 1: Single pulse maximum diffraction efficiency observed according to the temporal pulse width of the recorded beams at the constant energy per pulse of 30 mJ/cm$^2$.

Figure 2 presents the dynamic measurement of the diffraction efficiency according to the pulse temporal width. Since the diffraction increases by more than an order of magnitude between the nanosecond and the full-second excitation (see figure 1), we normalized the efficiency on this graph. It can be seen that the response of the material is quite different according to the energy delivery. Nanosecond and microsecond excitations give a sharp rise before achieving a maximum efficiency after about 100 milliseconds, well after the pulse is gone. However, the decay is faster in the case of the nanosecond pulse. For the 300 millisecond pulse, the rise time is much slower, where the diffraction increases during the entire time of the exposure and decreases immediately after the pulse is finished.
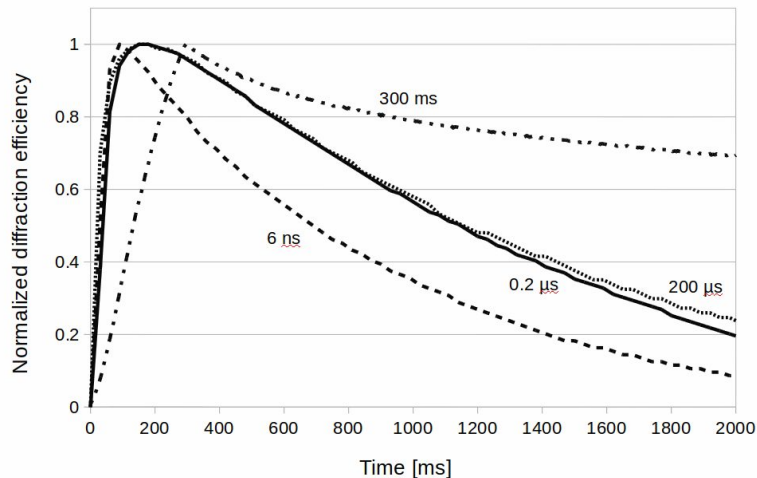
Figure 2: Dynamics of the normalized diffraction efficiency for different pulse temporal lengths at the constant energy per pulse of 30 mJ/cm$^2$.

## 3. DISCUSSION AND CONCLUSION

Recording the holographic grating in the PR device with pulsed laser light ranging from nanoseconds to one second showed very different diffraction efficiency and response dynamics. The diffraction efficiency monotonically decreases from 65% when recorded with a 1 second long pulse, to only 2% when recorded with a 20 microsecond pulse. At shorter pulse widths, the diffraction efficiency does not change anymore and stays around 2% down to the shortest pulse width of 6 ns.

There are 3 mechanisms that can be identified in the PR effect influencing the amplitude and dynamics of the material:
- Charge carrier photogeneration.
- Charge transport and trapping.
- Chromophore response.

The typical time scale for charge photogeneration by geminate recombination is usually much faster than the nanosecond time scale of our shortest pulse. [12] Therefore this process should not be influenced by the range of temporal pulse width we are accessing. On the other hand, charge transport and trapping that have been resolved by photoconduction time-of-flight have a characteristic time on the order of 0.1 to 5 milliseconds which is well within the extent of this measurement. [13] The chromophore response in our material is dependent on the DC fields, including the external bias field and the space-charge field, but not the radiative field. Consequently it should not be influenced by the recording pulse temporal width.

Accordingly, the measurement reported in figure 1 can be interpreted as follows: below 20 µs, the pulse excites the charges once and only once. Indeed, by the time the charge has migrated inside the bulk of the material and gets stuck in the closest trap available, the pulse is now gone and the entire material is in the dark. This means the charge has been trapped in a location regardless of if that location was in the bright or dark fringe of the interference pattern. This single excitation of the charge leads to a weaker diffraction efficiency due to the less than optimum charge distribution and index modulation. At longer and longer pulse temporal length, it is now possible for the charges that have been trapped in the bright region of the interference pattern to be re-excited by the tail of the pulse and move further away from the constructive interference regions of the illumination pattern. This re-excitation improves the charge distribution, concentrating the charge carriers in the dark regions, which better correspond to the original modulation of the intensity pattern and subsequently increases the diffraction efficiency.

This interpretation is equally supported by the dynamic measurements presented in figure 2. Indeed, the initial slope of the diffraction efficiency is quasi identical for the pulses shorter than 200 µs. This indicates that the process is not limited by photon delivery but by an intrinsic material property such as the photoconduction. For longer pulse lengths, such as 300 ms, the slope is much shallower and the diffraction keeps increasing during the entire time the sample is illuminated. The dynamics are now governed by the photon delivery and not the charge mobility. The slower decay time

observed at longer pulse length means the charges have to travel further away from where they are trapped to become recombined. This is because they have traveled further away from the region they have been generated and where the opposite charge carriers are still located.

In further works, we would like to compare the behavior we have observed in the present measurement with different pulse power, especially to compare the rise time according to the pulse energy. Also it will be very interesting to duplicate this experiment on other materials with faster or slower charge transport dynamics and to see if the diffraction efficiency is equally influenced by the pulse temporal length and/or where the inflection point is located.

Considering the holographic 3D display application, a videorate system involves the recording of at least 10,000 hogels per second. Excluding spatial multiplexing, this number of hogels requires a 10 kHz pulsed laser with each pulse writing a different hologram. The maximum pulse length at 10 kHz is 100 µs, so we need to find a PR material that has a decent diffraction efficiency at that pulse length. According to the present measurement, this means that we need a faster photoconductor. Such a material can be engineered by reducing the density of deep traps that slow down the charge transport. [11].

## REFERENCES

[1] S.A. Benton and V.M. Bove, Jr., Holographic imaging (Wiley-InterScience, New York, 2008).

[2] N.S. Holliman, N.A. Dodgson, G.E. Favalora, and L. Pockett, "Three-dimensional displays: a review and applications analysis," IEEE Trans. Broadcast. 57(2), 362–371 (2011).

[3] P.-A. Blanche et al., "Holographic three-dimensional telepresence using large-area photorefractive polymer," Nature 468(7320), 80–83 (2010).

[4] B. Lynn et al., "Recent advancements in photorefractive holographic imaging," J. Phys. Conf. Ser. 415, 012050 (2013).

[5] C. W. Christenson, et al., "Interdigitated coplanar electrodes for enhanced sensitivity in a photorefractive polymer", Optics Letters, Vol. 36, No. 17, September 1, 2011.

[6] B. Lynn et al., "Real-time imaging of chromophore alignment in photorefractive polymer devices through multiphoton microscopy", MRS Communications, vol. 15, issue 2, pp 243-250, (2015).

[7] H. Bjelkhagen, D. Brotherton-Ratcliffe, "Ultra-Realistic Imaging: Advanced Techniques in Analogue and Digital Colour Holography", CRC press, (2013).

[8] P.-A. Blanche, "Field guide to Holography", SPIE field guides volume FG31 (2014).

[9] J. Thomas *et al.*, "Bistriarylamine Polymer-Based Composites for Photorefractive Applications," *Adv. Mater.* **16**(22), 2032–2036 (2004).

[10] C. Christenson, "Improving Sensitivity of Photorefractive Polymer Composites", Ph.D. Thesis, University of Arizona, Department of Physics, (2011).

[11] B. Lynn, P.-A. Blanche, and N. Peyghambarian, "Photorefractive polymers for holography," *J. Polym. Sci. Part B Polym. Phys.* **52**(3), 193–231 (2014).

[12] T. M. Clarke and J. R. Durrant, "Charge Photogeneration in Organic Solar Cells", Chem. Rev. 110, 6736–6767, (2010).

[13] V. Coropceanu, et al., "Charge Transport in Organic Semiconductors", Chem.Rev., 107, 926−952, (2007).